Electronic Journal of Biotechnology 59 (2022) 62–73

Contents lists available at ScienceDirect

Electronic Journal of Biotechnology

www.elsevier.com/locate/ejbt

Research Article

Relationship between type II polyproline helix secondary structure and thermal hysteresis activity of short homopeptides

Roberto Rojas [a], Mónica Aróstica [b], Patricio Carvajal-Rondanelli [c], Fernando Albericio [d,e], Fanny Guzmán [f], Constanza Cárdenas [f,*]

[a] Instituto de Química, Facultad de Ciencias, Pontificia Universidad Católica de Valparaíso, Av. Universidad 330, Valparaíso, Chile
[b] Doctorado en Biotecnología, Pontificia Universidad Católica de Valparaíso y Universidad Federico Santamaría, Valparaíso, Chile
[c] Escuela de Alimentos, Facultad de Ciencias Agronómicas y de los Alimentos, Waddington 716, Pontificia Universidad Católica de Valparaíso, Chile
[d] Química Orgánica, Facultad de Química, Universidad de Barcelona and Centro de Investigación Biomédica en Red, Bioingeniería, Biomateriales y Nanomedicina (CIBER-BBN), Martí i Franqués 1, Spain
[e] School of Chemistry, University of KwaZulu-Natal, King Edward Avenue, Scottsville, Pietermaritzburg, South Africa
[f] Núcleo de Biotecnología Curauma, Pontificia Universidad Católica de Valparaíso, Av. Universidad 330, Valparaíso, Chile

GRAPHICAL ABSTRACT

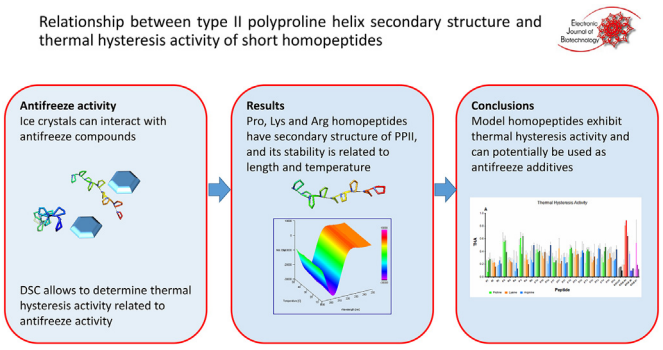

ARTICLE INFO

Article history:
Received 18 December 2021
Accepted 4 August 2022
Available online 9 August 2022

Keywords:
Antifreeze proteins
Antifreezing
Cationic homopeptides
Differential scanning calorimetry
Homopeptides
Ice-binding proteins
Ice recrystallization
Polyproline II helix

ABSTRACT

Background: Antifreezing activity is a phenomenon of great significance in food industry that affects the quality of frozen foods. As a solution, ice-binding proteins, more specifically antifreeze proteins, have been used to mitigate recrystallization. However, knowledge about the mechanism of ice recrystallization and the influence of antifreeze proteins is scarce.

Results: In this work, model homopeptides of three amino acids (proline, arginine and lysine) were studied by means of differential scanning calorimetry through the determination of their thermal hysteresis activity, to see the influence of several factors on their secondary structure. It was found that model homopeptides formed polyproline II type secondary structure that was more stable at low temperature. In addition, thermal hysteresis activity was higher for peptides of intermediate lengths and for proline homopeptides.

Conclusions: The study of homopeptides sheds light on the mechanism of antifreeze activity and will allow the design of new molecules with antifreeze properties to be used in diverse biotechnological fields.

Peer review under responsibility of Pontificia Universidad Católica de Valparaíso

* Corresponding author.
E-mail address: constanza.cardenas@pucv.cl (C. Cárdenas).

https://doi.org/10.1016/j.ejbt.2022.08.003

How to cite: Rojas R, Aróstica M, Carvajal-Rondanelli P, et al. Relationship between type II polyproline helix secondary structure and thermal hysteresis activity of short homopeptides. Electron J Biotechnol 2022;59. https://doi.org/10.1016/j.ejbt.2022.08.003.

1. Introduction

The phenomenon of recrystallization in ice that involves the growth of ice crystals at the expense of smaller ones strongly diminishes the quality of frozen foods during storage and shortens their shelf life [1,2,3,4]. This is a major concern in the production of ice cream and derived products, influencing their stability and quality [5,6,7,8].

An alternative to address this issue has been the use of ice-binding proteins (IBPs) [2,6,9,10], which in nature are the main effectors that inhibit ice formation. IBPs are present in a high diversity of organisms and can be grouped in antifreeze proteins (AFPs) and ice-nucleating proteins (INPs) [11]. Among AFPs, there is also a high variety of structures and proposed mechanism of action. Type I AFPs with an alpha-helical structure and some prevalence of repetitive motifs (with Thr, Asn and Asp predominantly), in which polar interactions occur through hydrogen bonding, appear to be a major mechanism of ice forming inhibition [12,13]. Type II AFPs have been described as globular proteins rich in cysteine domains; these AFPs have mixed secondary structures, similar to a calcium-dependent domain described in lectins, which would be responsible for ice binding [13,14]. Finally, Type III AFPs are also globular proteins whose interaction with ice occurs through specific regions or patches that form a flat surface that comes into contact with ice crystals [15]. The flat surface has patches containing hydrophilic residues (eg. Thr, Gln or Asn) which are conserved between isoforms [16,17,18]. As can be seen, the diversity of sequences and structures is wide and the mechanisms of action are not precisely defined. Additionally, an important property associated with antifreeze activity is thermal hysteresis that describes the ability to modify the freezing point of ice. This property is a characteristic of AFPs, and although has values that cover a wide spectrum between the different types of AFPs [11,19], it has been widely used to establish the antifreeze character of proteins and peptides with diverse applications [13,20,21].

An approach to shed light in the anti-freezing mechanism of AFPs is the use of model peptides with well-defined sequences and structures.

In this work, synthetic Pro, Arg and Lys homopeptides were used with length between 7 and 14 amino acid residues. These amino acids were chosen because of their tendency to form a polyproline II secondary structure and because their antifreezing properties have been reported [22,23,24,25]. The study of their interaction with ice was done by means of differential scanning calorimetry (DSC), through the determination of its thermal hysteresis activity as a measure of its antifreeze capacity [26,27].

It was found that the polyproline II secondary structure plays an important role in this interaction, which is correlated to the length of the peptide, being the peptides of intermediate length the ones presenting higher activity in terms of antifreezing activity. Also, the Pro homopeptides were those exhibiting the better features both in terms of secondary structure and interaction with ice [22].

Understanding the mechanism of antifreeze activity, beyond contributing to basic knowledge, is aimed to the design of new alternatives to be used in the food industry as an innovative, non-toxic and environmentally friendly option, among the many applications for antifreeze compounds [28].

2. Materials and methods

2.1. Synthesis of homopeptides

Synthesis reagents were purchased from Iris Biotech GmbH (Germany), and solvents were purchased from Merck KGaA (Germany).

Pro, Lys and Arg homopeptides between 7 and 14 amino acid residues, the three reference peptides: AQ4744 a fragment of a type I AFP, AQ4748 a short antifreeze peptide and AQ4751 a peptide from pig skin, and the peptide AQ1317 as negative control were synthesized by solid phase peptide synthesis (SPPS) using standard Fmoc/tBu strategy, following the tea bag protocol developed by Houghten [29]. Syntheses were performed according to protocols from previous works [30,31], in which Rink-amide 4-methyl benzhydrylamine resin (loading: 0.64 meq/g) was used with N,N,N′,N′-Tetramethyl-O-(1H-benzotriazol-1-yl) uronium hexafluorophosphate, O-(Benzotriazol-1-yl)-N,N,N′,N′-tetramethyluronium hexafluorophosphate (HBTU) and N,N-diisopropylethylamine (DIEA) activation, in dimethylformamide (DMF) as solvent.

Peptides were cleaved from the resin by using a mix of trifluoroacetic acid (TFA)/triisopropyl silane (TIS)/Milli-Q water (95/2.5/2.5 v/v). Desalting of crude peptides was performed using size-exclusion chromatography in Sephadex G10 resin using Milli-Q water as solvent [32]. The peptides were lyophilized and analyzed by reversed phase-high performance liquid chromatography (RP-HPLC, JASCO Corporation, Japan) to assess purity, and matrix-assisted laser desorption/ionization mass spectrometry (MALDI-TOF, Bruker Daltonics Inc., MA, USA) to confirm identity.

2.2. Circular dichroism spectroscopy

Circular dichroism (CD) spectra were obtained in a 1.0 mm path length quartz cuvette over 190–250 nm using a J-815 CD spectrometer coupled to a Peltier CDF-426S/15 (JASCO Corporation, Japan) with signal averaging over 2 s/nm interval in a concentration range of 1–2 mM with 30% v/v 2,2,2-trifluoroethanol (TFE) in ultrapure water. Three repeat scans were obtained for each sample, and the baseline spectrum was subtracted from the average. These spectra were obtained every 5°C between 5°C and 50°C and converted to molar ellipticity for a comparative study [30,33]. Additionally, control and reference peptides CD spectra were also recorded in pure water at 37°C.

2.3. Thermal hysteresis activity

Control and reference peptides and Pro, Lys and Arg homopeptides at 2, 10, 15 and 25 mM concentrations were analyzed in a differential scanning calorimeter DSC1 Star System (Mettler Toledo, Switzerland) implemented with a HSS8 high sensitivity sensor, and a Huber TC45 intracooler chiller (Offenburg, Germany) was used. The sensitivity of the DSC1 device is sub μW. A temperature

calibration was performed using indium before all calorimetric measurements.

The procedure was adapted from Zhang et al. [34]. Briefly, a 10 μL sample was placed in an aluminum pan and the weight of the sample was recorded using an analytical scale. An empty aluminum pan was placed in the reference cell. The sample was cooled from 10°C down to −25°C (completely frozen) at a rate of 3°C/min, then heated at a rate of 3°C /min up to −10°C, then slowly heated at a rate of 1°C /min until partially melted at a defined temperature (Tho) where the ice coexisted with the peptide solution; this temperature was maintained for 10 min to enhance the interaction between the peptide and the ice crystals, followed by a temperature decrease down to −10°C to observe the effect of the peptide on ice recrystallization. The sample was then cooled again to −25°C to completely refreeze it and finally heated at 3°C/min up to 10°C to ensure a return to initial conditions. To determine the Tho, two cooling curves are taken into account, one where recrystallization occurs and another where undercooling occurs and there is no recrystallization (an example of these curves can be seen in Fig. S1). The slight difference in temperature between these two curves guaranteed that in the Tho, there is a minimum amount of ice, so that the interaction with the peptide is maximum.

To compare the THA of the homopeptide series water was used as a blank [34,35], peptide AQ117 as a negative control (KKKKKKPKKKK) and three reference peptides: The first peptide, codified as AQ4744, is a fragment of a type I AFP (TAANAAAAAAA-TAR) that has been described to have THA [36]. The second peptide AQ4748 is a short antifreeze peptide (PTQTQTITGPR) reported with low THS but Ice recrystallization Inhibition (IRI) activity [35] and finally, a third peptide AQ4751 is a peptide derived from pig skin (GLLGPLGPRGLL), and described with a high THA [9].

The onset temperature (To) of recrystallization was recorded, and the thermal hysteresis activity (THA) was calculated by subtracting the onset temperature (To) from Tho.

A summary of the temperature program for DSC used in this study is shown in Table 1.

Two-way ANOVA followed by Dunnett's multiple comparisons test was performed using GraphPad Prism version 9.3.1 for MacOS, GraphPad Software, San Diego, California USA, https://www.graphpad.com.

3. Results

3.1. Secondary structure analysis

Homopeptide series were characterized by HPLC and mass spectrometry as reported in a previous work [30]. Information for the reference peptides is summarized in Table S1.

Type II polyproline helix (PPII) secondary structure is a right-handed helical structure with backbone dihedral angles φ and ψ of −75 and +145°, respectively [37]. In spectroscopy, this structure shows a minimum at 206 nm and a maximum at 220 nm. As can be seen, Pro (Fig. 1), Arg (Fig. 2) and Lys series homopeptides (Fig. 3) showed a polyproline II trend to different extents.

In the case of the Pro homopeptide series, the minimum and maximum have a red shift of 8–10 nm with respect to the typical polyproline structure due to the imino acid [38]; this homopeptide series showed the least dispersion with temperature in its secondary structure, and, by contrast, Arg homopeptide series exhibited the largest dispersion.

To study the relationship of secondary structure with temperature and peptide length, within each homopeptide series, two characteristic parameters were used: a comparison of the 220 nm maximum, and the PPII content calculated by Equation 1 [38,39].

$$\%PPII = \frac{[\theta]_{max} + 6100}{13700} \times 100 \qquad \text{Equation1}$$

where θ is the molar ellipticity value at 220 nm. In addition, the ratio between the residue ellipticity for the maximum and minimum $[\theta]_{220}/[\theta]_{206}$ at different temperatures was also compared.

The general behavior of the three homopeptide series (Pro, Arg, Lys) was the same as previously reported by our group [33]. Clearly, the minimum and maxima have higher absolute values at lower temperatures for each homopeptide series, and also for longer peptides. The PPII % for all three series was maximum at the lowest temperature and for the longest peptide, with values of 120.6% for Arg, 98.3% for Lys and 87.1% for Pro homopeptides (Table S2, Table S3 and Table S4). The minimum PPII % also coincided with the shortest peptide at the highest temperature for Lys (49.2%) and Pro (47.8%) series. In the case of Arg, minimum corresponded to 10 residues. Additionally, two different methods were used to analyze secondary structure content: CD-Pro-CONTIN [40,41] as implemented in spectra analysis of the J-815 CD spectrometer and BeStSEL server [42,43]. The database SP37A [44] was used as a reference for CDPro analysis since it includes five structural classes: alfa helix (H), beta strand (S), beta turn (T), polyproline II (PPII), and unordered structure (U). As can be seen with BestSel analysis (Table S5, Table S6 and Table S7), the "Others" structural class is the highest value in all the cases, and with CD-Pro almost all the cases the unordered structure represents > 40%, the other structural classes have varied values, being slightly higher those of T in polyproline series, and those of S in arginine and lysine series. The PPII in all cases was less than 20% (Table S8, Table S9 and Table S10).

CD spectra for reference peptides were recorded in water and 30% TFE. As can be seen, the structural tendency is the same in both cases (Fig. 4 and Table S1) and the effect of TFE is observed more clearly with peptide AQ4744, which has a α-helix tendency. Peptide AQ1317 has a PPII tendency; AQ4748 and AQ4751 have an unordered structure. Analysis of the spectra with CDPro showed the helix tendency for AQ4744, and the other three peptides pre-

Table 1
Temperature program for the differential scanning calorimetry. Steps 1, 2, 6 and 7 are the same for all samples, and the other steps (3 and 5) depend on the Tho found for each specific sample.

Step	Start temperature (°C)	Final temperature (°C)	Rate of change (°C/min)	Time (min)
1	10	−25	−3	11,7
2	−25	−10	3	5,0
3	−10	Tho*	1	specific†
4	Tho*	Tho*	0	10,0
5	Tho*	−10	−1	specific†
6	−10	−25	3	5,0
7	−25	10	3	11,7

* Specific Tho for each sample can be seen in supplementary Table S4.
† Specific time for each sample.

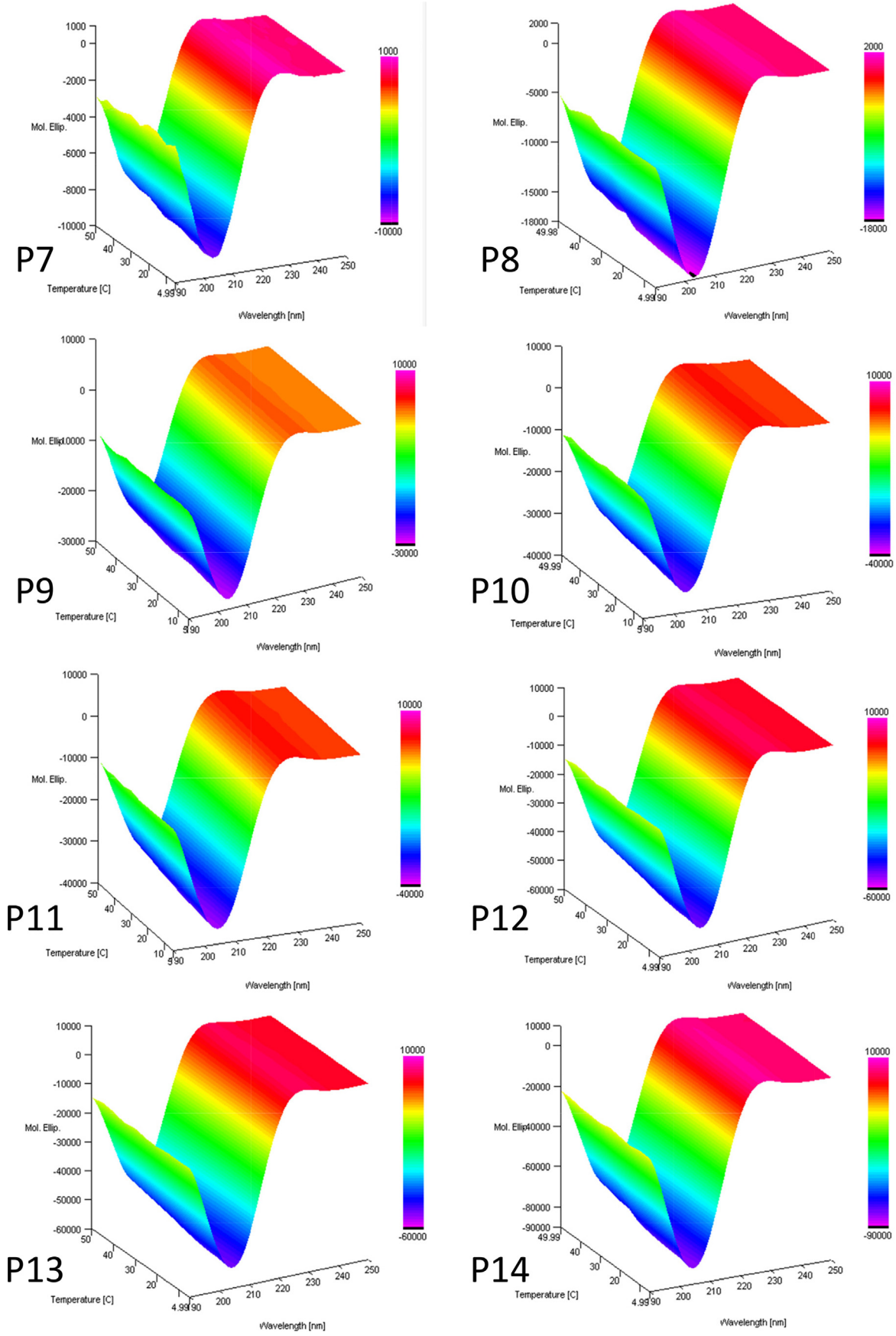

Fig. 1. Temperature-dependent CD spectra for proline homopeptides from 7 to 14 residues. Curves were recorded at a range of temperature between 5 and 50°C; the molar ellipticity values are indicated by the color scale.

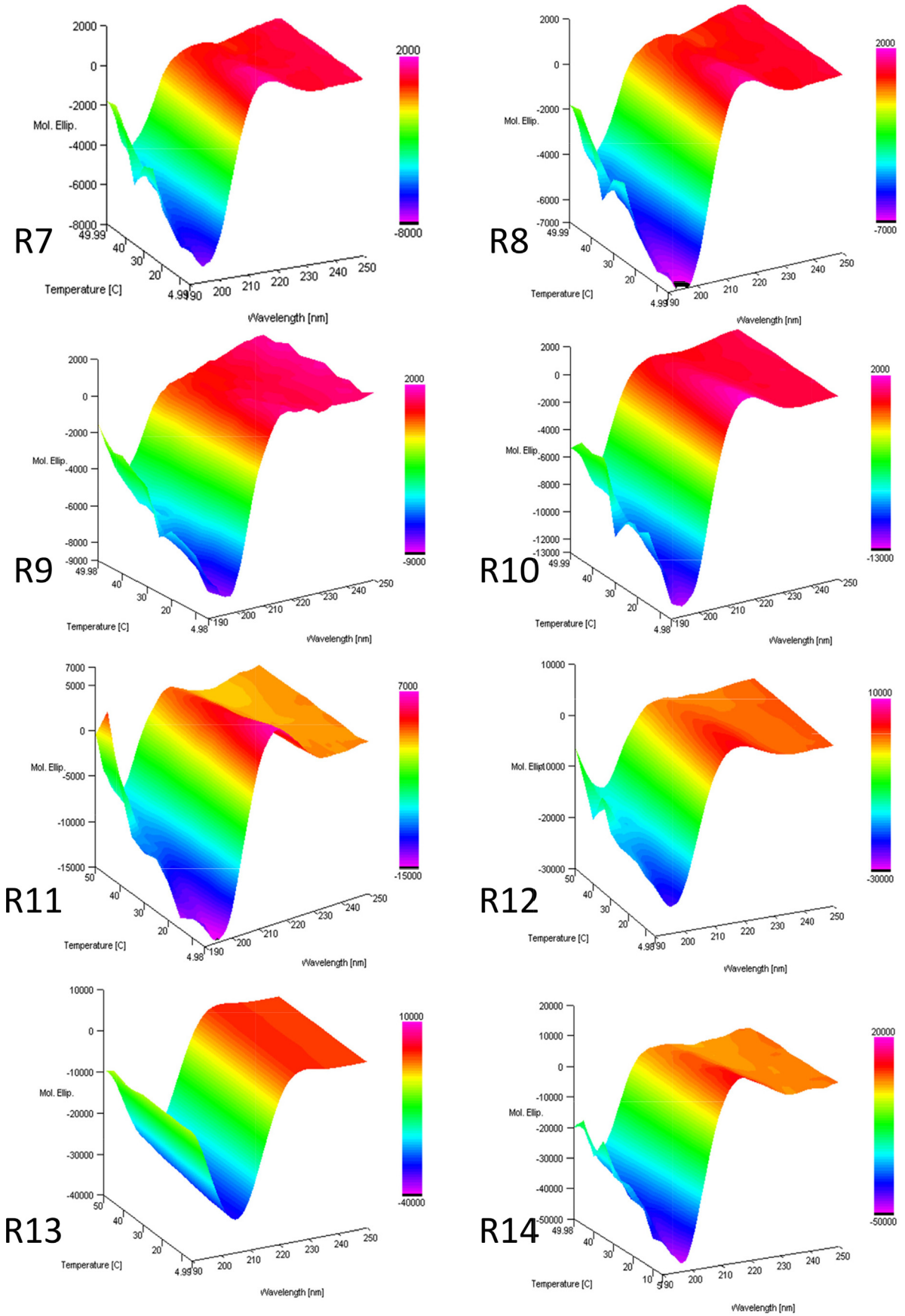

Fig. 2. Temperature-dependent CD spectra for arginine homopeptides from 7 to 14 residues. Curves were recorded at a range of temperature between 5 and 50°C; the molar ellipticity values are indicated by the color scale.

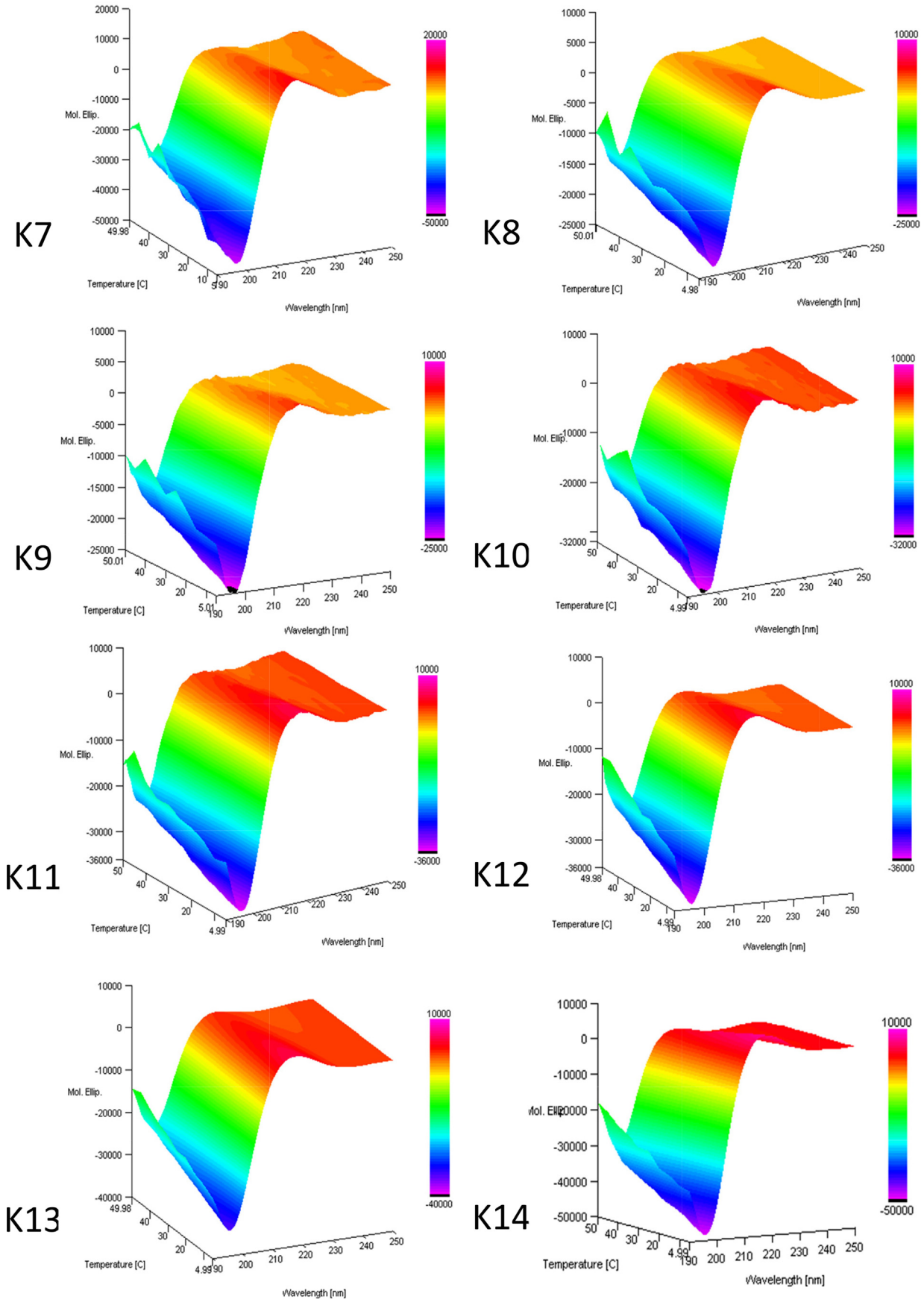

Fig. 3. Temperature-dependent CD spectra for lysine homopeptides from 7 to 14 residues. Curves were recorded at a range of temperature between 5 and 50°C; the molar ellipticity values are indicated by the color scale.

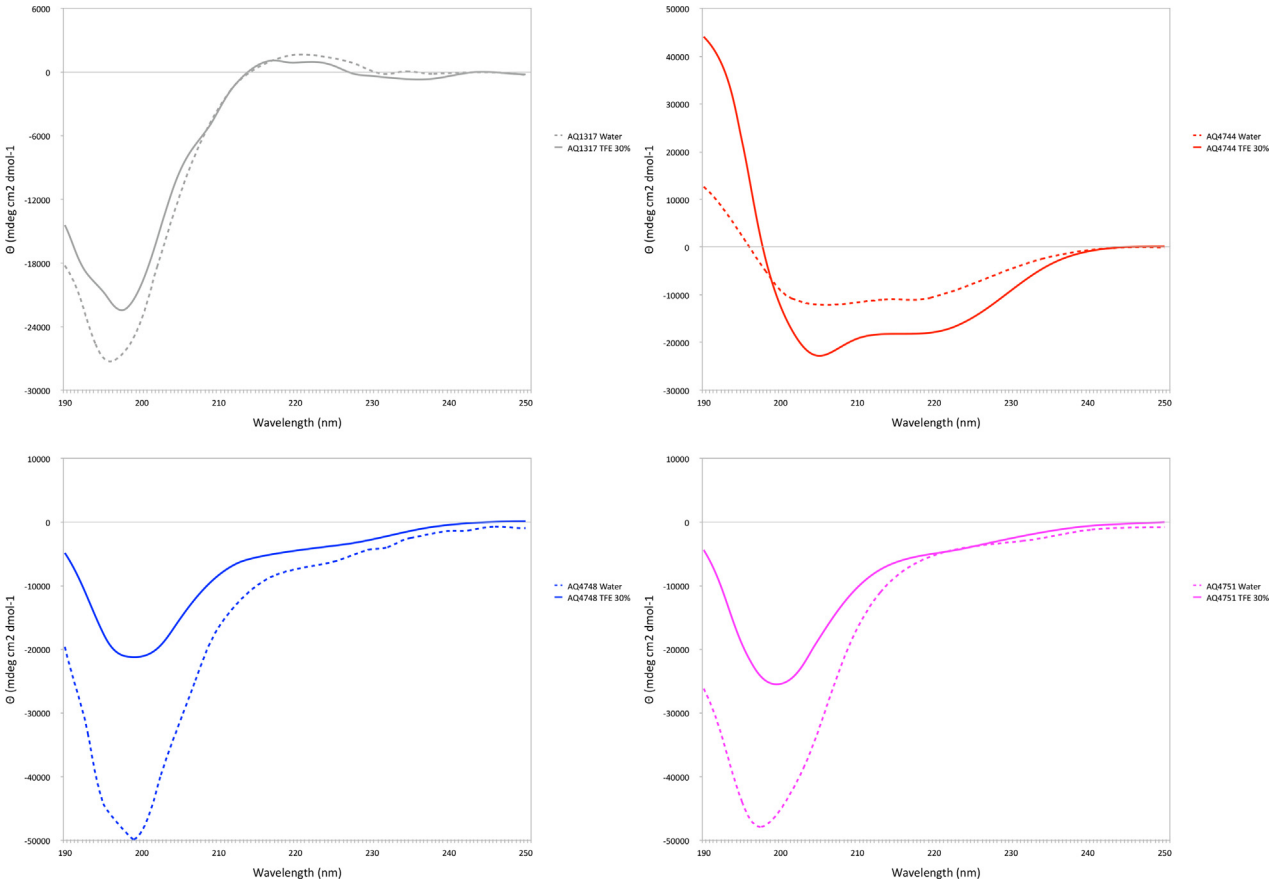

Fig. 4. CD spectra for reference peptides in water (dashed line) and in 30% TFE (solid line) at 37°C. Color code: AQ1317 grey, AQ4744 red, AQ4748 blue and AQ4751 magenta.

sent similar values to the homopeptides, and in the case of BeStSel server, the behavior is similar (Table S1).

In addition, the presence of an isodichroic point was observed in the temperature-dependent CD spectra, and also the $[\theta]_{220}/[\theta]_{206}$ ratio is nearly lineal for all the homopeptide series. This is interpreted as an indication of a balance between the PPII secondary structure and the disordered state [25].

This trend is clearer in the case of Pro homopeptides than in the case of Arg and Lys homopeptides (Fig. S2, Fig. S3, Fig. S4).

A structural model for the 7, 11 and 14 residues of the homopeptide series was constructed (Table 2) based on the P6 experimental structure [45].

3.2. Thermal hysteresis activity

Results of the DSC for each homopeptide series in terms of the THA (calculated as indicated in the methods section) are shown in Fig. 5. The Tho temperature for each peptide and the onset temperature are presented in Table S11.

Statistical analysis of the THA results was done by initially comparing the different concentrations for each peptide, observing only a few significant differences (Table S12). The activity of different peptides was compared with a negative control (AQ1317) at the different concentrations used. This analysis showed that almost all the series of homopeptides present a THA higher than that of the control (Fig. 4 and Table S13), with the homoproline series being the one that presented THA at all concentrations, with P8 and P9 having the best behavior.

Homoarginine series showed significant differences at 15 and 25 mM mainly, and homolysine series at 25 mM.

The THA values for any of the homopeptide series were in a similar range to that of the reference peptides and others reported in literature [9,35,36,48,49,50].

Although a pattern is not clearly observed, it is possible to observe THA in all the three homopeptide series, in a different extent in each one.

4. Discussion

Circular dichroism is widely used for the determination of secondary structure in proteins. However, the analysis methods to determine secondary structure have two major biases, to be applied to peptides, the first one is that the methods are built with protein databases, which present mixtures of secondary structures, and secondly, the defined structural classes are very limited, for which the analysis of CD in peptides is a developing area [51]. A specific case is the one that refers to polyproline II [38,52], which is the subject of this report. Its determination is based on the antecedents that exist in the literature and also on the experience gained in working with peptides.

Thus, in terms of secondary structure, Pro, Arg and Lys homopeptide series have been reported before as forming PPII structures, which are more stable at low temperature and for longer peptides [33,53], which is in agreement with what was found in the present study. It should be noted that equation 1, by which the %PPII was estimated, was determined from data with peptides that did not include arginine or lysine, and according to other reports, these two amino acids have a high propensity to form PPII, added to the flexibility they have compared to proline,

Table 2
Structural formula and 3D models for the 7, 11 and 14 residues of the homopeptide series. Formula was performed with Marvinsketch 20.21.0 (Chemaxon), and 3D structure was constructed with SpdbViewer [46] and Chimera [47] based in the experimental structure CCDC-1014542 from The Cambridge Crystallographic Data Centre [45].

Peptide	Structure
P7	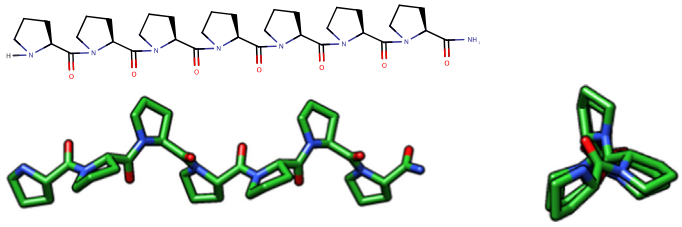
P11	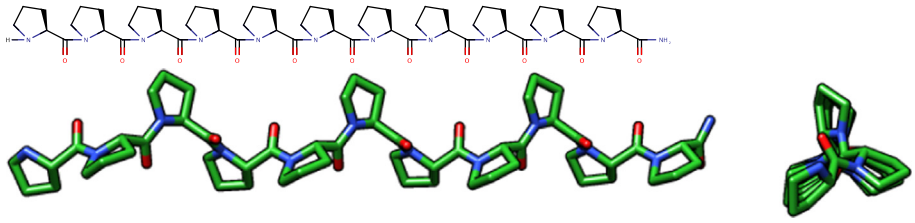
P14	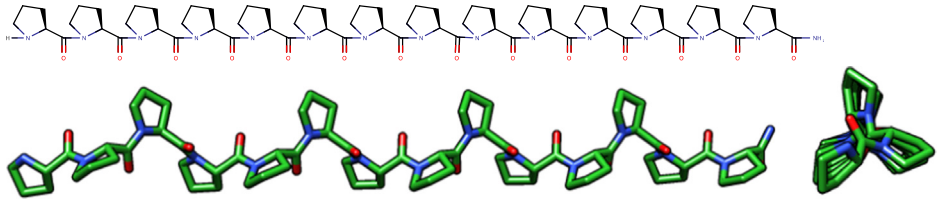
K7	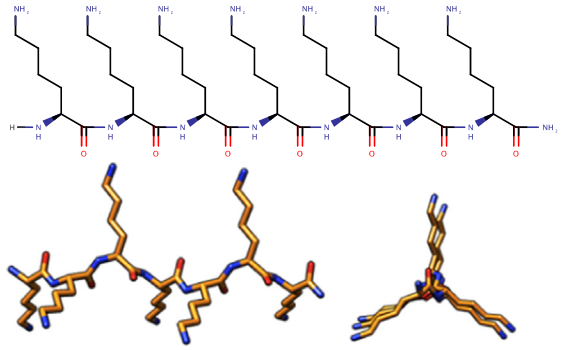
K11	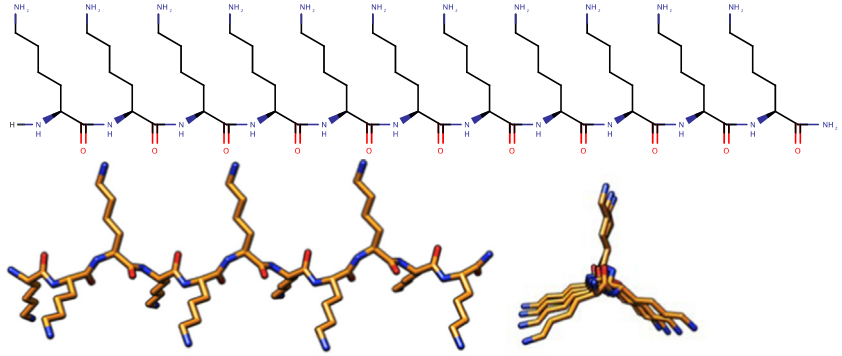
K14	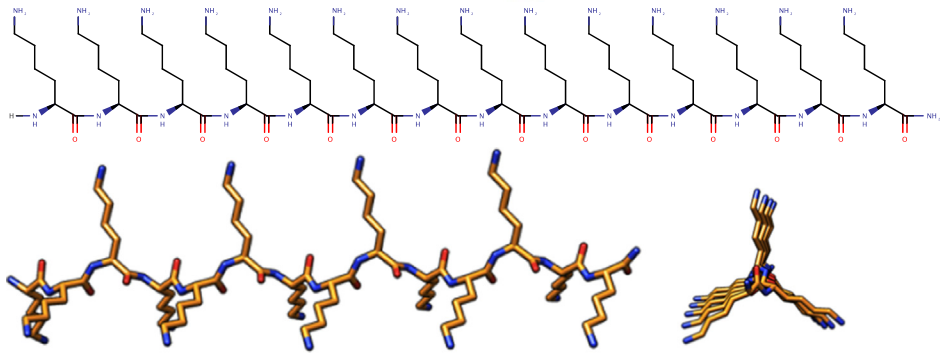

(*continued on next page*)

Table 2 (*continued*)

Peptide	Structure
R7	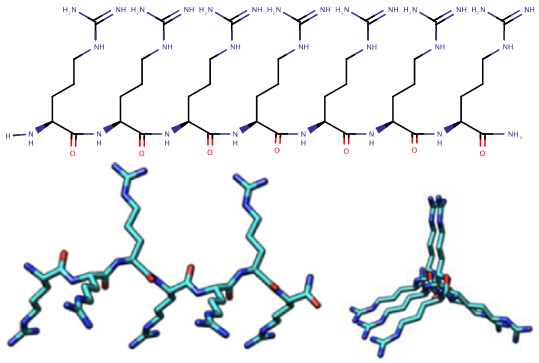
R11	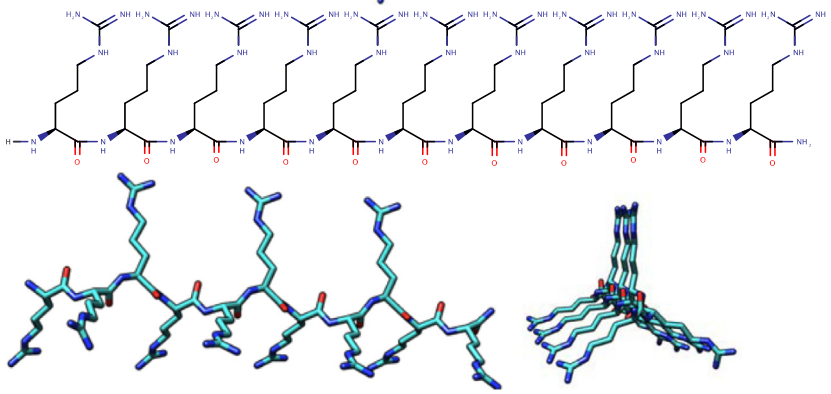
R14	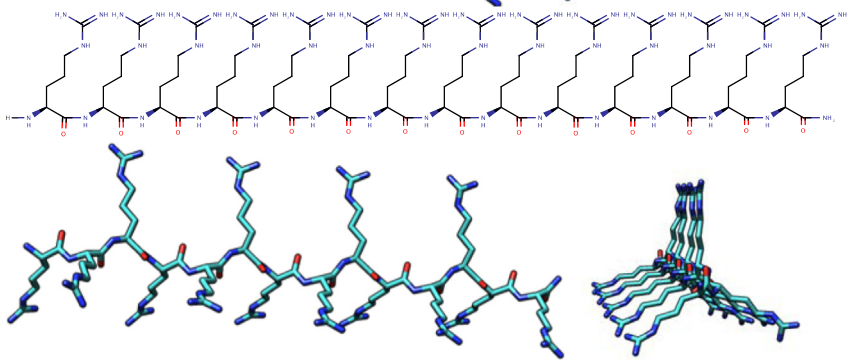

cause artifacts to exist, obtaining values of more than 100% for some cases (Table S4 and Table S7).

The mechanism of action of the antifreeze proteins (AFPs) and peptides and their role in their interaction with ice is a matter of debate [10,19,54]. There are many studies reporting different results and, until now, it has not been possible to define a general mechanism; however, there are some features to consider in the case of peptides:

1. Secondary structure, with a preference for PPII structure, has been reported to be important for the interaction with ice, and in particular with respect to their antifreeze activity [55,56]. It is postulated that the lack of intrachain hydrogen bonds can leave the peptide backbone available for interacting with ice, and this may be favored for amino acids with non-bulky side chains.
2. Length of the molecule is important: very short molecules or very long molecules affect the secondary structure of the peptide [57], also influencing their antifreeze capacity and decreasing their activity.

In this context, although almost all the synthetic homopeptides showed thermal hysteresis activity, it was higher in the homopeptides with an intermediate length, even though the PPII helix was favored in longer homopeptides. This can be explained as a combination between length and flexibility, with intermediate-size peptides having a defined structure, but also being flexible enough to interact with ice crystals, as is the case of P8 or P9 peptides, which showed activity at all concentrations tested. A similar behavior was observed for Arg homopeptides, R9 and R10 exhibiting the highest THA activity at 25 mM. Lys homopeptides were the less active series. It is possible that in the case of Lys and Arg homopeptides, their cationicity is the predominant feature on ice interaction, beyond the secondary structure, so that the interaction is different than with Pro homopeptides. Also, the electronic character of the guanidinium group of Arg, which can behave like a resonant structure, could modulate the interaction in a different way.

Interestingly, the peptide used as a negative control is a polylysine peptide with a proline in the middle of the chain and, although the secondary structure retains the PPII tendency, the THA decreases drastically. Of the three reference peptides, only one

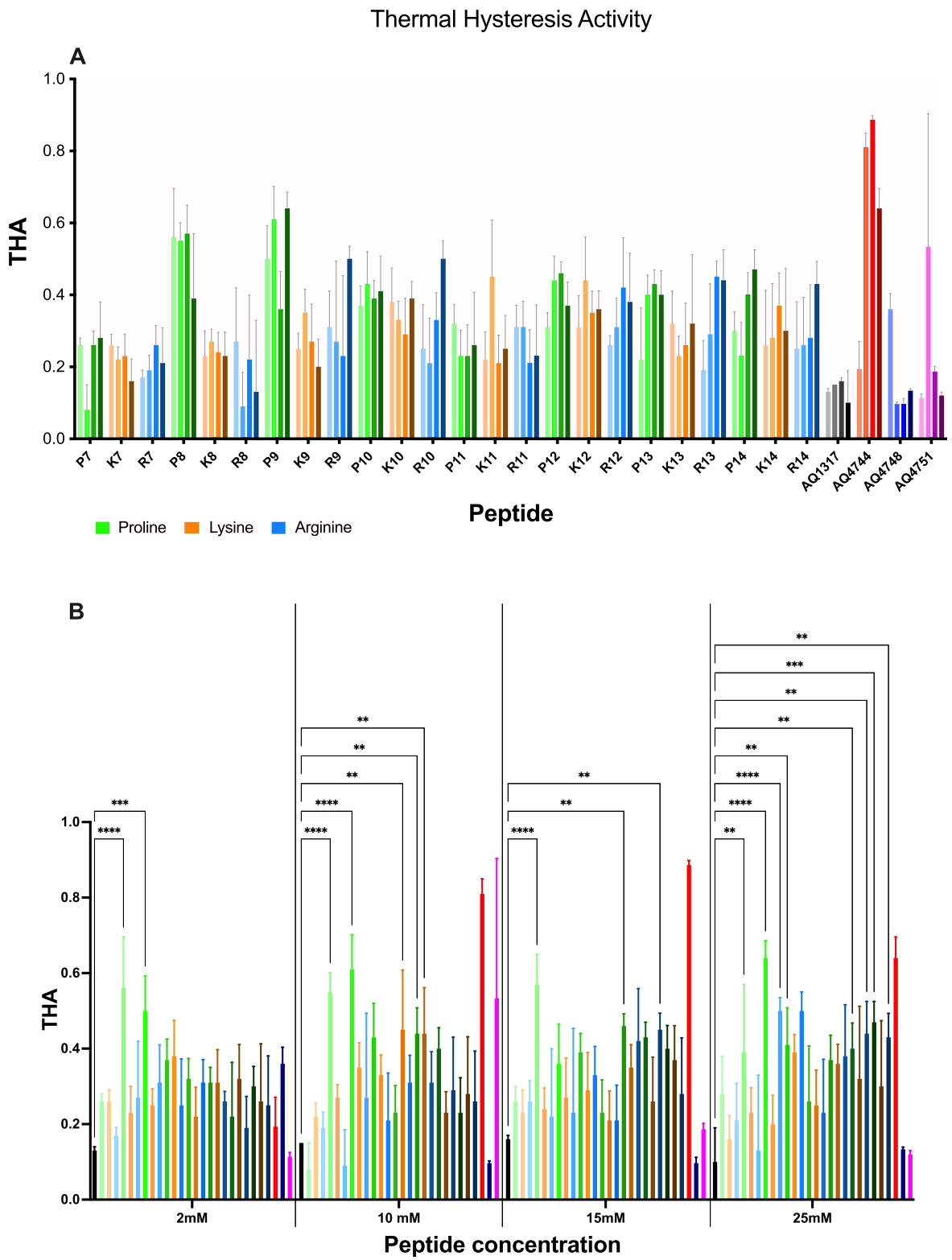

Fig. 5. Thermal hysteresis activity. A. The activity for homopeptide series and reference peptides at four different concentrations is presented. Color code is as follows: Lys series orange, Arg series blue, Proline series green. The peptide used as a negative control is in grey, and reference peptides are in red, blue and magenta. The colors are on a scale from light to dark depending on the concentration used: 2, 10, 15 or 25 mM. **B.** Comparison of the peptide vs AQ1317 (black bars) according to concentration. The homopeptide series are plotted in light to dark color according to the number of residues (7–14), and reference peptides are in red, dark blue and magenta. Significant differences are indicated at ** P < 0.01, *** P < 0.001, **** P < 0.0001.

behaved as reported. Peptide AQ4748 showed a random or disordered structure, and also low THA values. Peptide AQ4744 presents high values of THA and helix structure, unlike what was previously reported, which are low values of THA and a random structure. Likewise, peptide AQ4451 is reported with high values of THA, of the order of 5 C. It is possible that the differences may be related

to the methodology used, since there is not much detail about it in the cited references. The CD spectra of these peptides were performed in pure water and 30% TFE, which is a standard procedure, and as can be seen in Fig. 4, the secondary structure tendencies are conserved, being stabilized only those that present intrachain interactions, as previously reported [23,58].

It was impossible to establish a relationship between THA activity and peptide concentration, which may be due to a problem of measurement limitation or sensitivity with the technique used (DSC), so in future studies, the use of microcalorimetry as a complementary technique will be used to determine if this correlation exists.

5. Conclusions

Homopeptides of Pro, Lys and Arg between 7 to 14 residues showed a type II polyproline helix secondary structure, which is more clearly defined as the number of amino acid residues increases and as the temperature decreases, according to their molar ellipticity.

According to DSC, all homopeptides had antifreeze activity, with Pro homopeptides having the highest effect. Also, intermediate-length homopeptides favored the THA activity.

Studies with model peptides will allow the design of new molecules with antifreeze properties that could be used in a wide spectrum of applications in the food industry and in other biotechnological fields [9,10,13,59,60,61].

Author contributions

-Study conception and design: P Carvajal-Rondanelli, F Guzmán, F Albericio

- Data collection: R Rojas, M Aróstica

- Analysis and interpretation of results: R Rojas, M Aróstica, C Cárdenas

- Draft manuscript preparation: R Rojas, C Cárdenas

- Revision of the results and approved the final version of the manuscript: R Rojas, M Aróstica, P Carvajal-Rondanelli, F Albericio, F Guzmán, C Cárdenas.

Financial support

This work was funded through FONDECYT-Chile Grant 1210056.

Conflict of interest

The authors declare no conflict of interest.

Supplementary material

https://doi.org/10.1016/j.ejbt.2022.08.003.

References

[1] Roos YH. Glass Transition and re-crystallization phenomena of frozen materials and their effect on frozen food quality. Foods 2021;10(2):447. https://doi.org/10.3390/foods10020447. PMid: 33670558.

[2] Liu M, Liang Y, Wang Y, et al. Effects of recombinant carrot antifreeze protein from *Pichia pastoris* GS115 on the physicochemical properties of hydrated gluten during freeze-thawed cycles. J Cereal Sci 2018;83:245–51. https://doi.org/10.1016/j.jcs.2018.08.016.

[3] Chen X, Wu J, Li X, et al. Investigation of the cryoprotective mechanism and effect on quality characteristics of surimi during freezing storage by antifreeze peptides. Food Chem 2022;371:131054. https://doi.org/10.1016/j.foodchem.2021.131054. PMid: 34555708.

[4] Maity T, Saxena A, Raju PS. Use of hydrocolloids as cryoprotectant for frozen foods. Crit Rev Food Sci Nutr 2016;58(3):420–35. https://doi.org/10.1080/10408398.2016.1182892. PMid: 27171566.

[5] Damodaran S, Wang S. Ice crystal growth inhibition by peptides from fish gelatin hydrolysate. Food Hydrocoll 2017;70:46–56. https://doi.org/10.1016/j.foodhyd.2017.03.029.

[6] Kaleda A, Tsanev R, Klesment T, et al. Ice cream structure modification by ice-binding proteins. Food Chem 2018;246:164–71. https://doi.org/10.1016/j.foodchem.2017.10.152. PMid: 29291835.

[7] Piao Z, Park JK, Patel M, et al. Poly(L-Ala-*co*-L-Lys) exhibits excellent ice recrystallization inhibition activity. ACS Macro Lett 2021;10(11):1436–42. https://doi.org/10.1021/acsmacrolett.1c00584. PMid: 35549012.

[8] Soukoulis C, Fisk I. Innovative ingredients and emerging technologies for controlling ice recrystallization, texture, and structure stability in frozen dairy desserts: A review. Crit Rev Food Sci Nutr 2016;56(15):2543–59. https://doi.org/10.1080/10408398.2013.876385. PMid: 24593158.

[9] Cao H, Zhao Y, Zhu YB, et al. Antifreeze and cryoprotective activities of ice-binding collagen peptides from pig skin. Food Chem 2016;194:1245–53. https://doi.org/10.1016/j.foodchem.2015.08.102. PMid: 26471678.

[10] Cid FP, Rilling JI, Graether SP, et al. Properties and biotechnological applications of ice-binding proteins in bacteria. FEMS Microbiol Lett 2016;363(11):fnw099. https://doi.org/10.1093/femsle/fnw099. PMid: 27190285.

[11] Bar Dolev M, Braslavsky I, Davies PL. Ice-binding proteins and their function. Annu Rev Biochem 2016;85:515–42. https://doi.org/10.1146/annurev-biochem-060815-014546. PMid: 27145844.

[12] Chakraborty S, Jana B. Conformational and hydration properties modulate ice recognition by type I antifreeze protein and its mutants. Phys Chem Chem Phys 2017;18:11678–89. https://doi.org/10.1039/C7CP00221A. PMid: 28435965.

[13] Eskandari A, Leow TC, Rahman MBA, et al. Antifreeze proteins and their practical utilization in industry, medicine, and agriculture. Biomolecules 2020;10(12):1649. https://doi.org/10.3390/biom10121649. PMid: 33317024.

[14] Chakraborty S, Jana B. Calcium ion implicitly modulates the adsorption ability of ion-dependent type II antifreeze proteins on an ice/water interface: a structural insight. Metallomics 2019;11(8):1387–400. https://doi.org/10.1039/c9mt00100j. PMid: 31267120.

[15] Kar RK, Bhunia A. Biophysical and biochemical aspects of antifreeze proteins: Using computational tools to extract atomistic information. Prog Biophys Mol Biol 2015;119(2):194–204. https://doi.org/10.1016/j.pbiomolbio.2015.09.001. PMid: 26362837.

[16] DeLuca CI, Comley R, Davies PL. Antifreeze proteins bind independently to ice. Biophys J 1998;74(3):1502–8. https://doi.org/10.1016/S0006-3495(98)77862-2.

[17] Lee H. Effects of hydrophobic and hydrogen-bond interactions on the binding affinity of antifreeze proteins to specific ice planes. J Mol Graph Model 2019;87:48–55. https://doi.org/10.1016/j.jmgm.2018.11.006. PMid: 30502671.

[18] Lopez Ortiz JI, Quiroga E, Narambuena CF, et al. Thermal hysteresis activity of antifreeze proteins: A model based on fractional statistics theory of adsorption. Phys A Stat Mech Its Appl 2021;575:126046. https://doi.org/10.1016/j.physa.2021.126046.

[19] Biggs CI, Bailey TL, Graham B, et al. Polymer mimics of biomacromolecular antifreezes. Nat Commun 2017;8:1546. https://doi.org/10.1038/s41467-017-01421-7. PMid: 29142216.

[20] Ekpo MD, Xie J, Hu Y, et al. Antifreeze proteins: Novel applications and navigation towards their clinical application in cryobanking. Int J Mol Sci 2022;23(5):2639. https://doi.org/10.3390/ijms23052639. PMid: 35269780.

[21] Białkowska A, Majewska E, Olczak A, et al. Ice binding proteins: diverse biological roles and applications in different types of industry. Biomolecules 2020;10(2):274. https://doi.org/10.3390/biom10020274. PMid: 32053888.

[22] Esipova NG, Tumanyan VG. Omnipresence of the polyproline II helix in fibrous and globular proteins. Curr Opin Struct Biol 2017;42:41–9. https://doi.org/10.1016/j.sbi.2016.10.012. PMid: 27815983.

[23] Wierzbicki A, Knight CA, Rutland TJ, et al. Structure−function relationship in the antifreeze activity of synthetic alanine−lysine antifreeze polypeptides. Biomacromolecules 2000;1(2):268–74. https://doi.org/10.1021/bm000004w. PMid: 11710110.

[24] Rucker AL, Creamer TP. Polyproline II helical structure in protein unfolded states: Lysine peptides revisited. Protein Sci 2002;11(4):980–5. https://doi.org/10.1110/ps.4550102.

[25] Brown AM, Zondlo NJ. A propensity scale for type II polyproline helices (PPII): Aromatic amino acids in proline-rich sequences strongly disfavor PPII due to proline–aromatic interactions. Biochemistry 2012;51(25):5041–51. https://doi.org/10.1021/bi3002924. PMid: 22667692.

[26] Shtukenberg AG, Ward MD, Kahr B. Crystal growth with macromolecular additives. Chem Rev 2017;117(24):14042–90. https://doi.org/10.1021/acs.chemrev.7b00285. PMid: 29165999.

[27] Kristiansen E, Zachariassen KE. The mechanism by which fish antifreeze proteins cause thermal hysteresis. Cryobiology 2005;51(3):262–80. https://doi.org/10.1016/j.cryobiol.2005.07.007. PMid: 16140290.

[28] Baskaran A, Kaari M, Venugopal G, et al. Anti freeze proteins (Afp): Properties, sources and applications – A review. Int J Biol Macromol 2021;189:292–305. https://doi.org/10.1016/j.ijbiomac.2021.08.105. PMid: 34419548.

[29] Houghten RA. General method for the rapid solid-phase synthesis of large numbers of peptides: specificity of antigen-antibody interaction at the level of individual amino acids. Proc Natl Acad Sci USA 1985;82(15):5131–5. https://doi.org/10.1073/pnas.82.15.5131. PMid: 2410914.
[30] Guzmán F, Marshall S, Ojeda C, et al. Inhibitory effect of short cationic homopeptides against Gram-positive bacteria. J Pept Sci 2013;19 (12):792–800. https://doi.org/10.1002/psc.2578. PMid: 24243601.
[31] Guzmán F, Gauna A, Luna O, et al. The tea-bag protocol for comparison of Fmoc removal reagents in solid-phase peptide synthesis. Amino Acids 2020;52:1201–5. https://doi.org/10.1007/s00726-020-02883-8. PMid: 32851463.
[32] Valcárcel A, de las Heras M, Moses DF, et al. Comparison between Sephadex G-10 and Percoll for preparation of normospermic, asthenospermic and frozen/thawed ram semen. Anim Reprod Sci 1996;41(3–4):215–24. https://doi.org/10.1016/0378-4320(95)01453-5.
[33] Carvajal-Rondanelli P, Aróstica M, Marshall SH, et al. Inhibitory effect of short cationic homopeptides against Gram-negative bacteria. Amino Acids 2016;48:1445–56. https://doi.org/10.1007/s00726-016-2198-z. PMid: 26922474.
[34] Zhang C, Zhang H, Wang L, et al. Validation of antifreeze properties of glutathione based on its thermodynamic characteristics and protection of baker's yeast during cryopreservation. J Agric Food Chem 2007;55 (12):4698–703. https://doi.org/10.1021/jf070387q. PMid: 17508758.
[35] Kong LF, Qatran Al-Khdhairawi AA, Tejo BA. Rational design of short antifreeze peptides derived from *Rhagium inquisitor* antifreeze protein. Biocatal Agric Biotechnol 2020;23:101447. https://doi.org/10.1016/j.bcab.2019.101447.
[36] Kun H, Mastai Y. Activity of short segments of Type I antifreeze protein. Biopolymers 2007;88(6):807–14. https://doi.org/10.1002/bip.20844. PMid: 17868093.
[37] Adzhubei AA, Sternberg MJE, Makarov AA. Polyproline-II Helix in Proteins: Structure and Function. J Mol Biol 2013;425(12):2100–32. https://doi.org/10.1016/j.jmb.2013.03.018. PMid: 23507311.
[38] Lopes JLS, Miles AJ, Whitmore L, et al. Distinct circular dichroism spectroscopic signatures of polyproline II and unordered secondary structures: Applications in secondary structure analyses. Protein Sci 2014;23(12):1765–72. https://doi.org/10.1002/pro.2558. PMid: 25262612.
[39] Kelly MA, Chellgren BW, Rucker AL, et al. Host−guest study of left-handed polyproline II Helix Formation. Biochemistry 2001;40(48):14376–83. https://doi.org/10.1021/bi011043a. PMid: 11724549.
[40] Provencher SW, Gloeckner J. Estimation of globular protein secondary structure from circular dichroism. Biochemistry 1981;20(1):33–7. https://doi.org/10.1021/bi00504a006. PMid: 7470476.
[41] van Stokkum IHM, Spoelder HJW, Bloemendal M, et al. Estimation of protein secondary structure and error analysis from circular dichroism spectra. Anal Biochem 1990;191(1):110–8. https://doi.org/10.1016/0003-2697(90)90396-Q.
[42] Micsonai A, Wien F, Bulyáki É, et al. BeStSel: a web server for accurate protein secondary structure prediction and fold recognition from the circular dichroism spectra. Nucleic Acids Res 2018;46:W315–22. https://doi.org/10.1093/nar/gky497. PMid: 29893907.
[43] Micsonai A, Wien F, Kernya L, Lee Y-H, Goto Y, Réfrégiers M, et al. Accurate secondary structure prediction and fold recognition for circular dichroism spectroscopy. Proc Natl Acad Sci 2015:112. https://doi.org/10.1073/pnas.1500851112. PMid: 26038575.
[44] Sreerama N, Woody RW. Estimation of protein secondary structure from circular dichroism spectra: Comparison of CONTIN, SELCON, and CDSSTR methods with an expanded reference set. Anal Biochem 2000;287(2):252–60. https://doi.org/10.1006/abio.2000.4880. PMid: 11112271.
[45] Wilhelm P, Lewandowski B, Trapp N, et al. A crystal structure of an oligoproline PPII-Helix, at last. J Am Chem Soc 2014;136(45):15829–32. https://doi.org/10.1021/ja507405j. PMid: 25368901.
[46] Guex N, Peitsch MC. SWISS-MODEL and the Swiss-Pdb Viewer: An environment for comparative protein modeling. Electrophoresis 1997;18 (15):2714–23. https://doi.org/10.1002/elps.1150181505. PMid: 9504803.
[47] Pettersen EF, Goddard TD, Huang CC, et al. UCSF Chimera - A visualization system for exploratory research and analysis. J Comput Chem 2004;25 (13):1605–12. https://doi.org/10.1002/jcc.20084. PMid: 15264254.
[48] Deng J, Apfelbaum E, Drori R. Ice growth acceleration by antifreeze proteins leads to higher thermal hysteresis activity. J Phys Chem B 2020;124 (49):11081–8. https://doi.org/10.1021/acs.jpcb.0c08119. PMid: 33232147.
[49] Nishimiya Y, Kondo H, Takamichi M, et al. Crystal structure and mutational analysis of Ca^{2+}-independent type II antifreeze protein from longsnout poacher, *Brachyopsis rostratus*. J Mol Biol 2008;382(3):734–46. https://doi.org/10.1016/j.jmb.2008.07.042 PMid: 18674542.
[50] Wu J, Rong Y, Wang Z, et al. Isolation and characterisation of sericin antifreeze peptides and molecular dynamics modelling of their ice-binding interaction. Food Chem 2015;174:621–9. https://doi.org/10.1016/j.foodchem.2014.11.100. PMid: 25529728.
[51] Ezerski JC, Zhang P, Jennings NC, et al. Molecular Dynamics ensemble refinement of intrinsically disordered peptides according to deconvoluted spectra from circular dichroism. Biophys J 2020;118(7):1665–78. https://doi.org/10.1016/j.bpj.2020.02.015. PMid: 32145192.
[52] Corcilius L, Santhakumar G, Stone RS, et al. Synthesis of peptides and glycopeptides with polyproline II helical topology as potential antifreeze molecules. Bioorganic Med Chem 2013;21(12):3569–81. https://doi.org/10.1016/j.bmc.2013.02.025. PMid: 23523384.
[53] Tiffany ML, Krimm S. Effect of temperature on the circular dichroism spectra of polypeptides in the extended state. Biopolymers 1972;11(11):2309–16. https://doi.org/10.1002/bip.1972.360111109. PMid: 4634868.
[54] Duman JG. Animal ice-binding (antifreeze) proteins and glycolipids: an overview with emphasis on physiological function. J Exp Biol 2015;218 (12):1846–55. https://doi.org/10.1242/jeb.116905. PMid: 26085662.
[55] Mochizuki K, Molinero V. Antifreeze glycoproteins bind reversibly to ice via hydrophobic groups. J Am Chem Soc 2018;140(14):4803–11. https://doi.org/10.1021/jacs.7b13630. PMid: 29392937.
[56] Carvajal-Rondanelli PA, Marshall SH, Guzman F. Antifreeze glycoprotein agents: structural requirements for activity. J Sci Food Agric 2011;91 (14):2507–10. https://doi.org/10.1002/jsfa.4473. PMid: 21725975.
[57] Urbańczyk M, Góra J, Latajka R, et al. Antifreeze glycopeptides: from structure and activity studies to current approaches in chemical synthesis. Amino Acids 2017;49:209–22. https://doi.org/10.1007/s00726-016-2368-z. PMid: 27913993.
[58] Roccatano D, Colombo G, Fioroni M, et al. Mechanism by which 2,2,2-trifluoroethanol/water mixtures stabilize secondary-structure formation in peptides: A molecular dynamics study. Proc Natl Acad Sci 2002;99 (19):12179–84. https://doi.org/10.1073/pnas.182199699. PMid: 12196631.
[59] Kim H, Lee J, Hur Y, et al. Marine antifreeze proteins: structure, function, and application to cryopreservation as a potential cryoprotectant. Mar Drugs 2017;15(2):27. https://doi.org/10.3390/md15020027. PMid: 28134801.
[60] de la Cruz-Gavia A, Pérez-Alonso C, Barrera-Díaz CE, et al. Survival of *Saccharomyces cerevisiae* microencapsulated with complex coacervate after freezing process. Food Hydrocoll 2018;82:45–52. https://doi.org/10.1016/j.foodhyd.2018.03.045.
[61] Correia LFL, Alves BRC, Batista RITP, et al. Antifreeze proteins for low-temperature preservation in reproductive medicine: A systematic review over the last three decades. Theriogenology 2021;176:94–103. https://doi.org/10.1016/j.theriogenology.2021.09.025. PMid: 34600433.